Multidisciplinary Characterization of Novel Emulsion Polymers

Morgan Sibbald*, Laurand Lewandowski, Michael Mallamaci, Ed Johnson

Goodyear Chemical, The Goodyear Tire & Rubber Company, 1485 East Archwood Ave., Akron, Ohio 44306

SUMMARY: A series of novel emulsion styrene-butadiene copolymer blends were characterized using a multidisciplinary approach involving both analytical and rheological measurements. The blends were composed of 50/50 w/w high molecular weight (ca. 800,000 Da) ESBR and low molecular weight (ca. 200,000 Da) ESBR, each component having a different bound styrene level. When the difference in bound styrene between the two components was greater than 18%, a two phase co-continuous morphology was observed by scanning probe microscopy, consistent with two glass transitions measured by temperature modulated DSC. Molecular weight and molecular weight distributions were characterized by both size exclusion chromatography and thermal field flow fractionation with multiangle light scattering detection. ThFFF was unique in its ability to detect ultra-high molecular weight (> 10^7 Da) fractions suggesting that traditional SEC often under-estimates polymer molecular weight . Blending polymers of different molecular weights and styrene levels resulted in reduced molecular weight between entanglements which, based on rheological measurements, would be expected to improve processability.

Introduction

Styrene-butadiene rubber (SBR) produced by emulsion polymerization has been a critical material for the tire industry since World War II. Recent developments of new SBRs and other tire elastomers have focused primarily on anionic solution polymerization. Unlike free-radical initiated emulsion methods, solution methods allow control of molecular weight (MW), molecular weight distribution (MWD), microstructure, sequence distribution and branching.[1-3)] Synthetic control over the molecular architecture helps target desirable material properties including elasticity, abrasion resistance, tensile strength, elongation, modulus, interaction with fillers and processability.

 CCC 1022-1360/00/$ 17.50+.50/0

The blending of emulsion styrene-butadiene rubbers (ESBR) has been considered as a means to obtain solution polymer-like properties. Blends of SBR[4], natural rubber/SBR[5] or cis-butadiene rubber with SBR[6] or natural rubber[7] have been previously reported. In the present work, a series of novel elastomers were prepared by blending a high molecular weight ESBR with a low molecular weight ESBR, each having a unique styrene content. The blends were characterized using a multidisciplinary approach that combined analytical and rheological information in order to develop a detailed understanding of the polymer structure-property relationships.

Materials

The polymers characterized in the current study are listed in Table 1. Samples A, B and 1712C are typical emulsion polymers. Blends are designated by the nomenclature "xx/yy" where the high molecular weight component has a styrene content of "xx" and the low molecular weight component has a styrene content of "yy". The blends were prepared by mixing approximately 50/50 weight percent ratios of the two latexes to a target Mooney viscosity (ML1'+4') of 50 and then coagulating the rubber. All emulsion SBRs were prepared on the laboratory scale except Goodyear Plioflex 1712C which is a commercial product. Duradene 751 is a solution-polymerized SBR (SSBR) manufactured by the Firestone Synthetic Rubber & Latex Company and was used to compare ESBR and SSBR properties.

Morphology of Polymer Blends

Temperature-modulated differential scanning calorimetry was used to estimate the glass transition temperatures (Tg) of the single component polymers and polymer blends. Glass transition values were taken as the extrapolated onset of the heat capacity dependent or reversing heat flow curve. Experiments were conducted using a 2 ^{o}C/min linear heating rate with a modulation amplitude of ±1.5 ^{o}C, modulation period of 60 s and a helium purge at 25 mL/min. Polymer blends consisted of a high molecular weight component having about 23.5% bound styrene and a low molecular weight component having from 0% bound styrene (polybutadiene) to 79% bound

Table 1. Average styrene content and thermal properties of SBRs.

Sample	Average Bound Styrene / %	Mooney Viscosity [a]	Tg (1) / °C	Tg (2) / °C
A	23	105	-55	
B	50	14	-19	
23/0	12	47	-58	-80
23/5	9	53	-61	-75
23/23	23	56	-57	
23/34	28	48	-54	
23/50 [b]	37	54	-56	-20
23/65	44	49	-55	5
23/79	51	51	-55	36
1712C [c]	23	49	-55	
SSBR [c]	25	45	-61	

[a] ASTM Standard Test Method D 1646-96a.
[b] Sample is a blend of polymers A and B.
[c] Polymers contain approximately 27% weight/weight of a low MW aromatic oil which lowers the Mooney viscosity relative to the raw polymer.

styrene. When the difference in bound styrene between the two components of a given blend was greater than 18%, two Tg's were identified (Table 1). For example, blend 23/50 which had a difference in bound styrene of 27% between the two components, had Tg's at –56 °C and –20 °C. The fact that these Tg's in the blend are the same as the Tg's for the isolated single components (data not shown) indicates the polymers are incompatible. Any interaction between the components would be expected to shift the Tg's relative to the pure materials. A single Tg was observed when the styrene difference was less than 18%, e.g. samples 23/23 and 23/34. The components of the blends in these materials appeared to be completely miscible. Livingston and Rongone previously found that SBR blends formed heterogeneous mixtures when the styrene difference between the components was greater than 20%,[4] consistent with the current study.

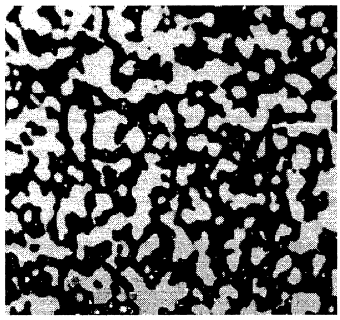

Fig. 1: Scanning probe micrograph of ESBR blend 23/50 showing two phase co-continuous morphology. Image size 10 μm^2.

The morphology of the blends was characterized using a Digital Instruments NanoScope® Multimode™ scanning probe microscope (SPM) operated in the TappingMode™. An image from the surface of blend 23/50 is shown in Fig. 1. The presence of two polymer domains is obvious. Each domain comprised about 50% of the scanned area, as expected from the 50/50 weight/weight blend ratio. A major advantage of SPM over temperature modulated DSC was the ability to visually show the relative sizes and shapes of the two domains that were only suggested by calorimetry.

The contrast in Fig. 1 is given by phase-lag differences across the material surface. Elings et al. have demonstrated that phase lag is a function of energy dissipation that occurs during the scanning tip-to-material surface interaction.[8)] This energy dissipation can be related to the mechanical properties of the surface. A two phase co-continuous morphology was observed for all blends having a difference in bound styrene between the two components of greater than 18%.

By measuring the phase-lag signatures of the single components from blend 23/50, the lighter color or bright phase in Fig. 1 was found to be the 50% styrene-containing polymer. A relationship was discovered between the phase lag difference between the two components of a given blend and the bound styrene difference. The linear dependence between phase lag and styrene level is depicted in Fig. 2. The authors believe this is one of the first reports identifying a quantitative relationship between phase lag and polymer viscoelasticity.

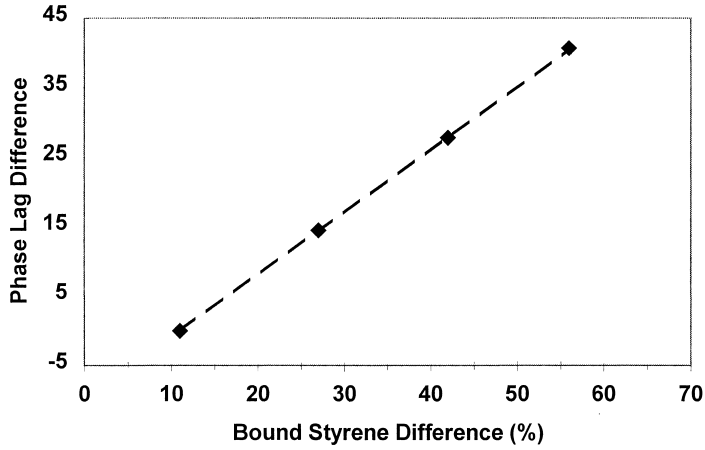

Fig. 2: Phase lag difference as a function of bound styrene difference in the ESBR blends. Differences were calculated as component 1 minus component 2.

Polymer Molecular Weights

Multidetector size exclusion chromatography was used to characterize the polymer molecular weights and molecular weight distributions. The combination of a refractive index (RI) concentration detector with a Wyatt Technologies MiniDAWN multiangle light scattering (LS) detector provided absolute molecular weights without the need for traditional calibration. Samples were dissolved in tetrahydrofuran (THF) and chromatographed using two columns, a Polymer Laboratories Plgel Mixed B and a Plgel Mixed C, at a flow rate of 1.0 mL/min. All samples were injected through 1.0 μm pore size syringe filters. Chromatograms for sample SSBR and blend 23/50 are shown in Fig. 3a and b, respectively. In both samples, the LS detector response peaks at a shorter elution time than the RI response. This behavior is attributed to the light scattering dependence on both molar mass and concentration,[9] whereas the differential refractive index depends only on concentration. Figs. 3a and b also depict the calculated molar mass versus elution time profiles. As expected for SEC, these profiles show a linear decrease in MW with increasing elution time.

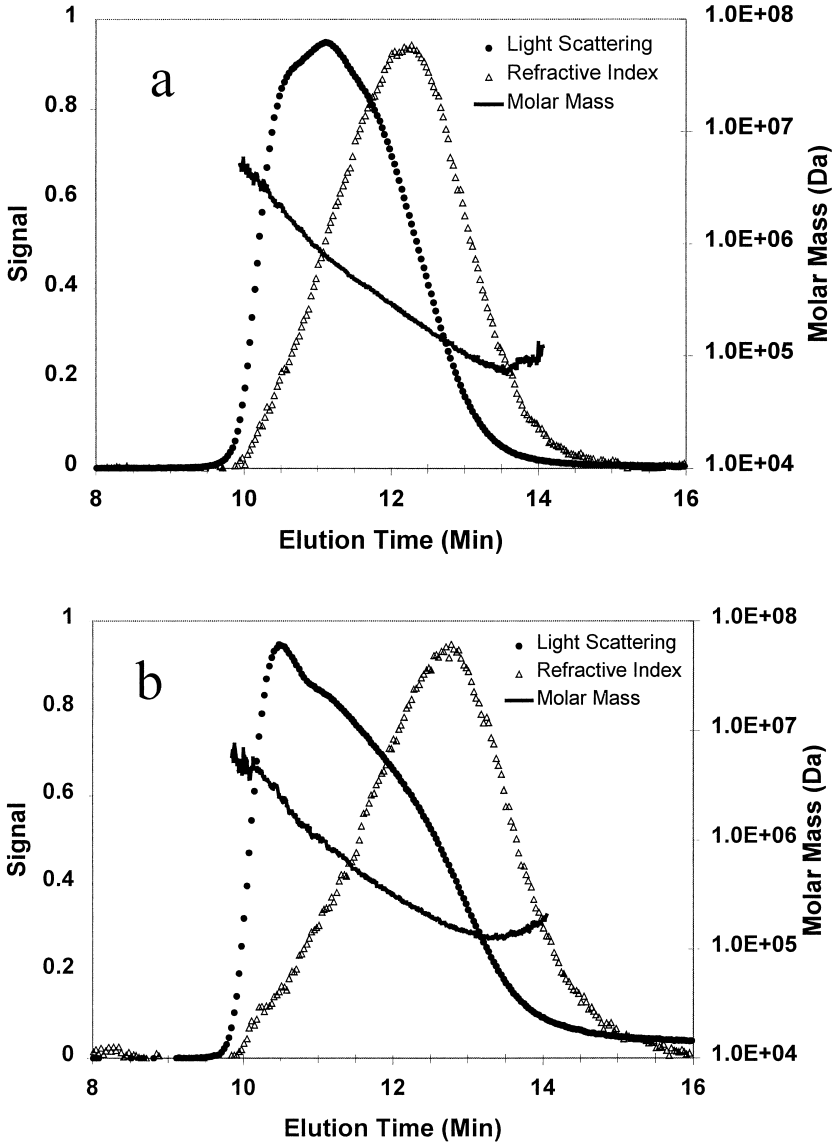

Fig. 3: Size exclusion chromatograms and calculated molar mass versus retention time for (a) solution SBR and (b) emulsion SBR blend 23/50.

The SEC results are summarized in Table 2; blends 23/0, 23/5, 23/23, 23/34, 23/65 and 23/79 were all similar to blend 23/50 and are not reported. Sample A and the commercial sample 1712C were both polymerized to a target Mooney viscosity of 105 and, as expected, had similar MWs and MWDs. However, there was some concern about whether these two samples were truly the same, given the fact that the mass recoveries were quite different. A mass recovery less than 100% reflects material lost to the required sample filtration for SEC and column effects including adsorption on the packing material.[10] The lower mass recovery for sample A may be due to higher levels of soluble gel, i.e. highly entangled or crosslinked polymer chains. Furthermore, the 41% mass recovery of sample A suggests that SEC may be significantly underestimating the average molecular weight. Mass recoveries closer to 100% and what are believed to be more representative average MWs were obtained for the lower MW emulsion SBRs and the solution SBR. The 96% mass recovery of the SSBR reflects the tighter control of MW by anionic polymerization compared to typical free radical polymerizations.

Fulton and Groves recently have shown that multi-detector thermal field flow fractionation (ThFFF) is better than SEC for characterizing synthetic and natural rubbers.[11] MWs up to 10^9 Da were observed by ThFFF. In this technique, a dissolved sample is injected unfiltered onto a narrow flow channel, shown

Table 2. SEC results from selected emulsion and solution SBR polymers.

Sample	Weight-Average MW / Da	MWD [a]	Mass Recovery of Polymer / % [b]
A	770,000	1.5	41
B	230,000	2.7	98
23/50	390,000	1.7	84
1712C	810,000	1.5	68
SSBR	520,000	2.3	96

[a] Ratio of weight average to number average molecular weight.
[b] Calculated using the calibrated refractive index concentration detector and the known injected mass.

schematically in Fig.4. Two parallel plates separated by a 127 μm thick polyimide spacer form the channel. A thermal gradient is generated between the plates by heating the upper plate to a defined temperature while maintaining the lower plate temperature using a recirculating chiller. This thermal gradient provides a force to drive molecules toward the lower plate, or low temperature wall. Fractionation is achieved based on differences in thermal conductivity. Laminar flow provides a second mechanism of fractionation, separating molecules based on hydrodynamic size. Larger molecules and those having a larger thermal conductance generally elute from the channel late. The ThFFF system in the present work consists of a FFFractionation, LLC Model T-100 Polymer Fractionator coupled to a conventional refractive index detector and a Wyatt Technology DAWN DSP 18-angle laser light scattering photometer capable of determining accurate molecular weights for higher MW polymers.[9)]

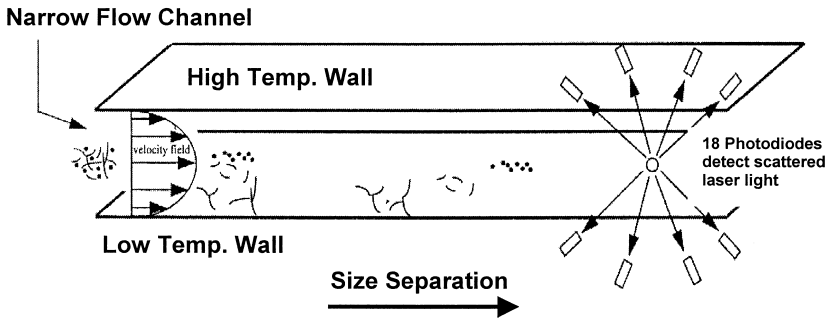

Fig. 4: Schematic of the thermal field flow fractionation system. Multiangle laser light scattering and differential refractive index are used for detection.

The ThFFF fractogram for sample SSBR is shown in Fig. 5a. Also shown is the calculated molar mass profile as a function of elution time. Note that the order of elution is opposite to that observed by SEC – lower molecular weight materials elute first. The narrow peak that eluted around 1.5 min (off-scale on vertical axis) is due to the low molecular weight extending oil. The remaining broad peak is attributed to the polymeric fraction. Because the sample was injected unfiltered into an open channel,

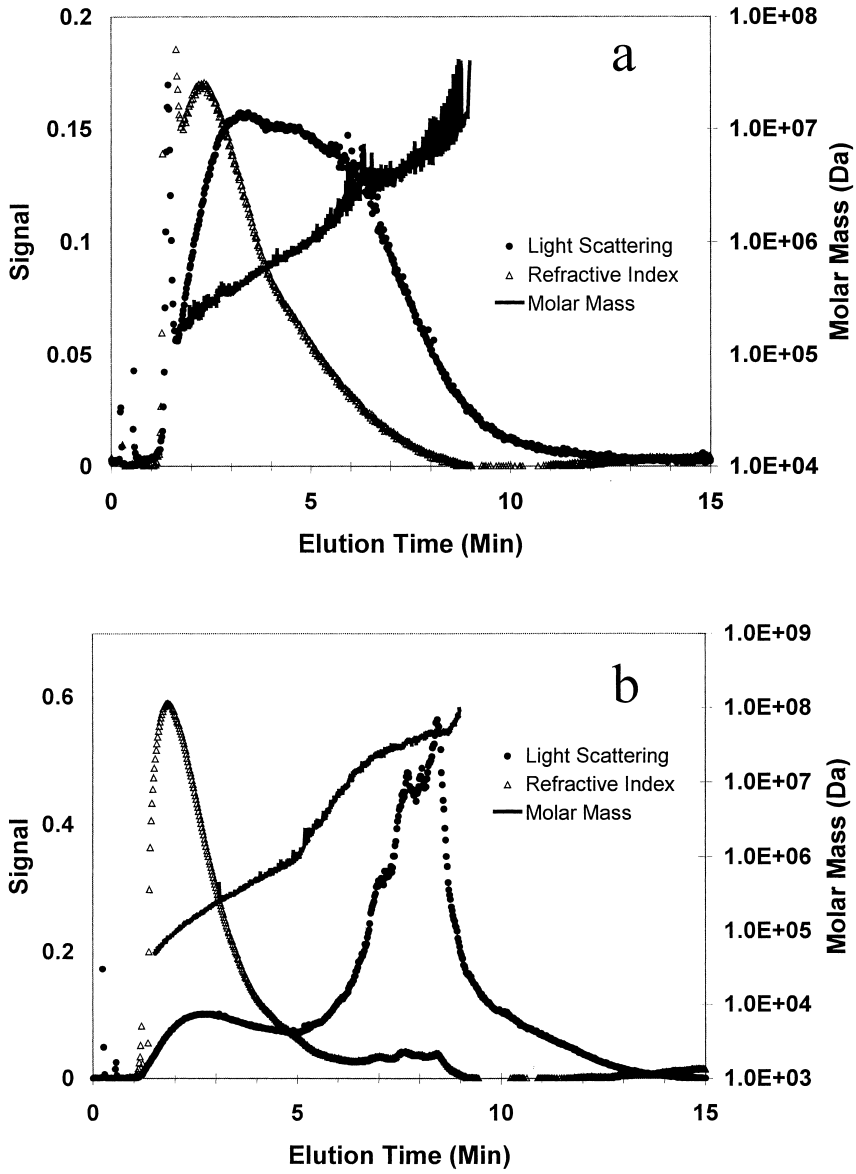

Fig. 5: Thermal field flow fractionation raw detector signals and calculated molar mass as a function of elution time for (a) solution SBR and (b) emulsion SBR blend 23/50. THF solvent at 0.6 mL/min. ThFFF power programmed method using initial delta temperature of 60 ^{o}C, final delta temperature of 0 ^{o}C after 30 min. Polymer samples were 0.12 mg injected unfiltered.

one can reasonably assume 100% mass recovery. The calculated molecular weight increased only slightly from 520,000 Da by SEC to 670,000 Da by ThFFF. Also, the fact that both LS and RI detectors reached baseline around 10 min is indicative of a relatively monodisperse molecular weight distribution, supporting the fact that anionic polymerization provides good control over MWD.

A more intriguing ThFFF fractogram was obtained for the ESBR blend 23/50 (Fig. 5b). As the RI concentration response approached baseline around 5 min, an unusual, strong LS peak appeared. This strong LS peak is due to an ultra-high molecular weight fraction that the authors believe has not been previously identified in such ESBRs. Note the increase in the slope of the calculated molar mass versus elution time profile at 5 min. At longer elution times, the molar mass neared 10^8 Da. The weak refractive index signal indicates that the high molecular weight peak accounted for only about 10% of the injected polymer mass. By analyzing 100% of the polymer, the weight average MW increased from 390,000 Da by SEC to over 2,000,000 Da by ThFFF. When blend 23/50 was injected into the ThFFF through a 1.0 μm syringe filter, as used for SEC analyses, the ultra-high molecular weight fraction was substantially reduced (Fig. 6). This further emphasizes the contention that SEC can underestimate the MW of certain polymers. The ultra-high molecular weight

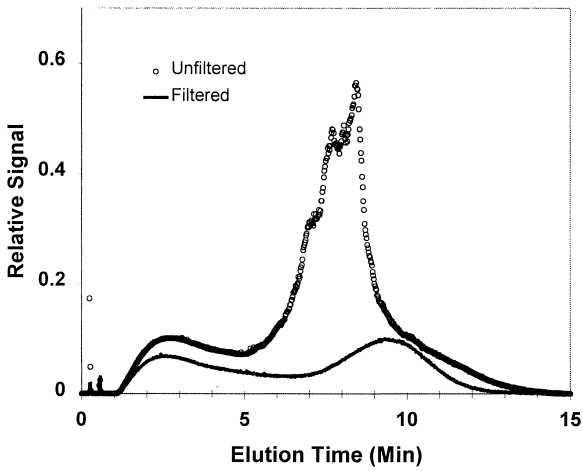

Fig. 6: Effect of filtering the ESBR blend 23/50 sample for thermal field flow fractionation. Conditions as in Fig.5.

fractions found in these emulsion SBRs contribute to a very broad molecular weight distribution and are expected to noticeably impact the viscoelastic properties of the material.

Rheological Characterization

Dynamic oscillatory measurements were used to characterize the viscoelastic behavior of the single components and polymer blends near the rubbery plateau and terminal regions of the mastercurve. The terminal region is particularly important for predicting polymer processability (i.e. ease of mixing, milling, extrusion, etc.).[12] Mastercurves were constructed from data obtained from frequency sweeps from 0.01 Hz to 100 Hz at three different temperatures (50 ^{o}C, 80 ^{o}C and 120 ^{o}C) and then shifting the data using time-temperature superposition.[13]

Polymer chains in the solid state tend to become entangled, forming a network. Strains imposed at high frequencies (e.g. 100 rad/s) do not allow sufficient time for the chains to disentangle. Instead, the chain segments between entanglements rearrange storing elastic energy as a result of the entropy change.[12] This storage of elastic energy results in a higher storage modulus (G') relative to the loss modulus (G") and is referred to as the rubbery plateau region of the mastercurve. As the oscillation frequency is decreased, the chain segments eventually have sufficient time to flow through the points of entanglement. The lack of constraints reduces the ability of the material to store elastic energy resulting in G' decreasing relative to G". The cross-over of G' and G" indicates the transition from the rubber plateau to the terminal flow region where the slope of G' is proportional to the square of the angular velocity (ω^2) and G" is proportional to ω. The mastercurve for sample B, a low molecular weight ESBR, is given in Fig. 7. The cross-over of G' and G" was observed in the neighborhood of 0.1 rad/s. The terminal relaxation time or time required for the last polymer chain to disentangle and flow was estimated to be around 10 s, based on the 0.1 rad/s cross-over frequency.

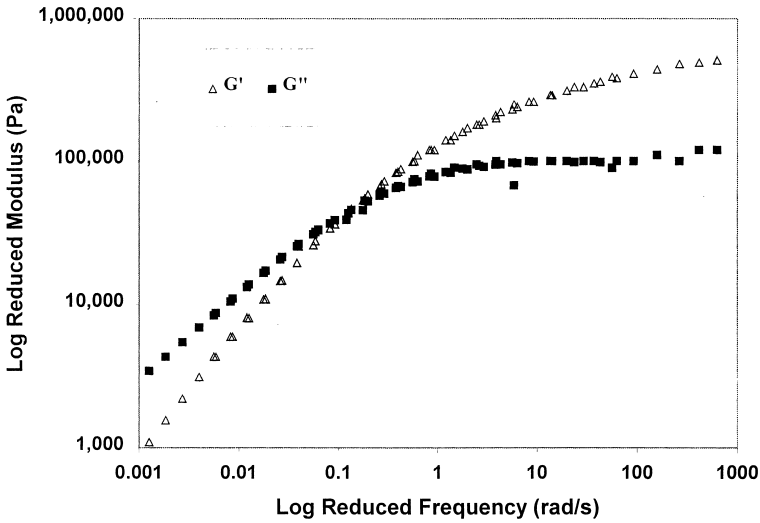

Fig. 7: Reduced storage modulus (G') and loss modulus (G") as a function of frequency for ESBR polymer B. Reference temperature = 50 °C.

The mastercurve for sample A, a high molecular weight ESBR, is shown in Fig. 8a. Unlike sample B, the transition from the rubbery plateau to the terminal region of the mastercurve, appears to lie outside of the frequency range of the curve. The G' and G" curves were parallel at low frequencies (e.g. 0.1 rad/s) resulting in no cross-over. This behavior is attributed to high molecular weight chains having extremely long relaxation times, estimated to be greater than 1000 s. These chains are the ultra-high molecular weight fraction detectable by ThFFF.

The commercial polymer 1712C was shown to have a similar polymeric-fraction MW and MWD to sample A, but it contains 27% w/w of a low molecular weight aromatic oil. The mastercurve for 1712C is given in Fig. 8b. The oil functions as a plasticizer to lower the modulus, relative to oil-free rubber, making it easier to process. However, there is still a significant amount of ultra-high molecular weight polymer in the material resulting in long terminal relaxation times. This manifests itself in the lack of a cross-over in the mastercurve.

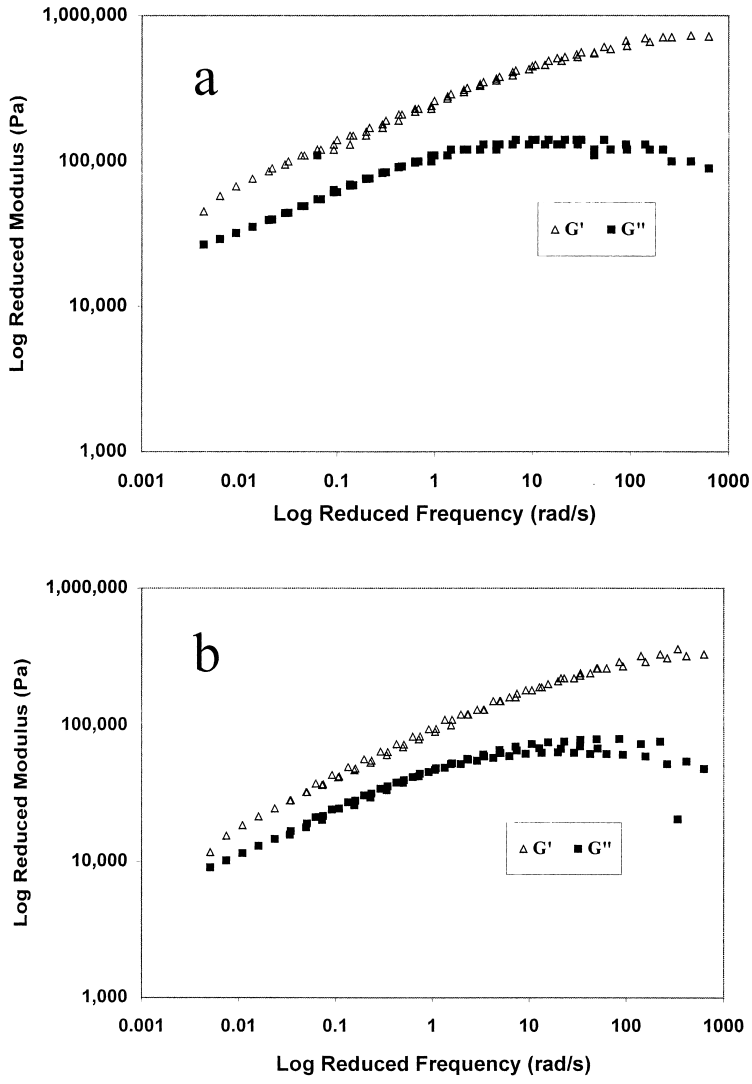

Fig. 8: Reduced storage modulus (G') and loss modulus (G") as a function of frequency for ESBR (a) sample A and (b) sample 1712C. Reference temperature = 50 ^{o}C.

The blends of high and low MW rubber were prepared in an attempt to improve the processability or flow properties of a 50 Mooney viscosity ESBR. The blends characterized in this work appeared to be directionally better than the benchmark, sample A. Unlike sample A, the mastercurve for blend 23/50 was found to have a cross-over at 0.01 rad/s (Fig. 9). Note that 0.01 rad/s is an order of magnitude lower than that observed for sample B which results from the higher average MW of blend 23/50. The presence of a cross-over in this higher molecular weight, 50 Mooney viscosity polymer is a good indicator of improved processability. Comparing frequency sweeps of all blends, the frequency at cross-over was found to have a linear dependence on the difference in bound styrene contents of the two blend components (Fig. 10). This dependence can be attributed to the average molecular weight between entanglements. For a given SBR polymer chain, the styrenic chain segments are less mobile than the butadiene chain segments and, therefore, have a lower probability for entanglements. The lower probability for entanglements results in a material with better flow properties, thus a higher frequency at cross-over of the storage modulus and loss modulus curves.

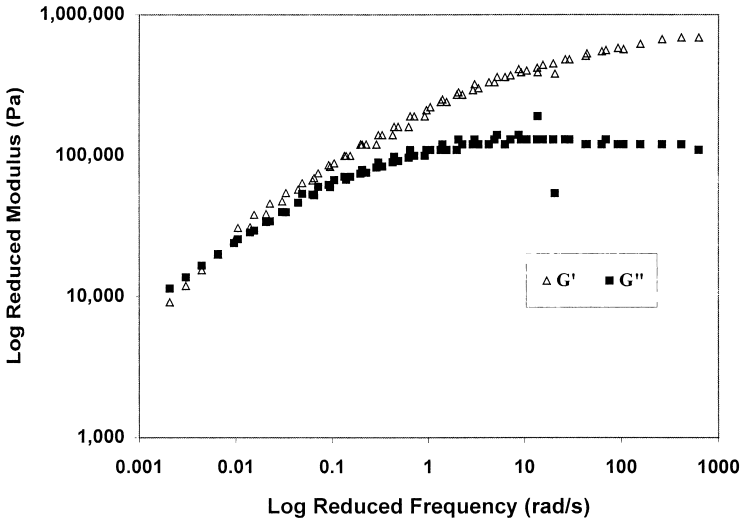

Fig. 9: Reduced storage modulus (G') and loss modulus (G") as a function of frequency for ESBR blend 23/50. Reference temperature = 50 ^{o}C.

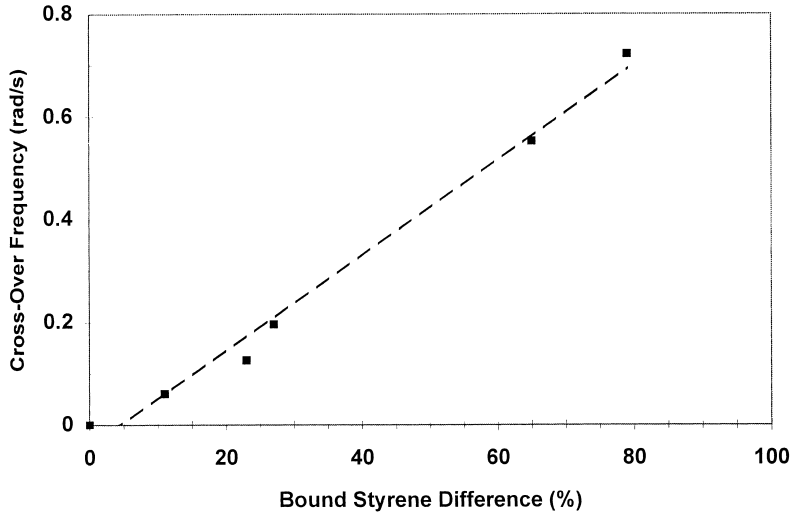

Fig. 10: Frequency at cross-over of storage modulus (G') and loss modulus (G") as a function of bound styrene difference between the two components of the ESBR blends.

It is particularly interesting that both the rheological behavior and the phase lag difference from scanning probe microscopy exhibited similar dependence on styrene levels of the polymers. Both analyses are measures of energy dissipation. However, rheological testing is sensitive to the bulk material viscoelasticity while microscopy is unique in its ability to probe energy dissipated at the material surface through a combination of viscoelastic, adhesive and frictional mechanisms.

Conclusion

Blends of two different emulsion styrene-butadiene copolymers were found to be incompatible when the difference in styrene compositions was greater than 18%. This was suggested by thermal analysis which identified two glass transitions at the same temperatures as the pure components. Scanning probe microscopy was able to confirm incompatibility by visually showing a two-phase, co-continuous morphology. Multidetector size exclusion chromatography was found to significantly underestimate the molecular weight of the emulsion polymers, particularly those

having Mw's greater than 250,000 Da. Better characterization of the molecular weight and molecular weight distribution was achieved using thermal field flow fractionation with multi-angle light scattering detection. ThFFF identified significant fractions of ultra-high molecular weight material that may be inherent to the free radical-initiated SBR emulsion polymerization process. An ultra-high molecular weight fraction was not observed in a typical anionic solution polymerized SBR for tire applications. The effect of molecular weight and bound styrene differences on the viscoelastic properties was readily apparent. The blends demonstrated a cross-over of the storage modulus and loss modulus near the terminal flow region of the viscoelastic spectrum, similar to lower molecular weight polymers. This has implications for improved processability of the blends compared to current commercial ESBRs.

Acknowledgments

The authors would like to express their sincere appreciation to The Goodyear Tire & Rubber Company for permission to publish this work. The authors also wish to thank Mark Altman for the thermal analysis measurements and data interpretation.

References

1. S. L. Aggarwal, I. G. Hargis, R. A. Livigni, H. J. Fabris, and L. F. Marker, in: *Advances in Elastomers Rubber Elasticity*, J. Lal and J. E. Mark (Eds.), Plenum, New York 1986, p. 17
2. C. C. Chang, A. F. Halasa, J. W. Miller, Jr., and W. L. Hsu, *Polym. Int.*, **33,** 151 (1994)
3. H. L. Hsieh and R. P. Quirk, *Anionic Polymerization: Principles and Practical Applications*, Marcel Dekker, New York 1996
4. D. I. Livingston and R. L. Rongone, presented at the 5th International Rubber Conference, Brighton, England, 1968, 337
5. D. C. Blackley and R. C. Charnock, *J. Inst. Rubber Ind.*, **7,** 60 (1973)
6. GB 1045980 (1966), Japan Synthetic Rubber Co.
7. R. N. Kienle, E. S. Dizon, T. J. Brett, and C. F. Eckert, *Rubber Chem. Technol.*, **44,** 996 (1971)
8. J. P. Cleveland, B. Anczykowski, A. E. Schmid, and V. B. Elings, *Appl. Phys. Lett.*, **72,** 2613 (1998)
9. P. J. Wyatt, *Anal. Chim. Acta,* **272,** 1 (1993)
10. S. Lee, *J. Microcolumn Sep.*, **9,** 281 (1997)
11. W. S. Fulton and S. A. Groves, *J. Nat. Rubb. Res.*, **12,** 154 (1997)
12. J. D. Ferry, *Viscoelastic Properties of Polymers*, Wiley, New York 1980
13. M. L. Williams, R. F. Landel, and J. D. Ferry, *J. Am. Chem. Soc.*, **77,** 3701 (1955)